Environmental Pollution 259 (2020) 113836

Contents lists available at ScienceDirect

Environmental Pollution

journal homepage: www.elsevier.com/locate/envpol

Monitoring polymer degradation under different conditions in the marine environment☆

Ana Beltrán-Sanahuja [a, *], Nuria Casado-Coy [b], Lorena Simó-Cabrera [c], Carlos Sanz-Lázaro [c, d]

[a] Analytical Chemistry, Nutrition & Food Sciences Department, University of Alicante, 03690, Alicante, Spain
[b] Marine Sciences and Applied Biology Department; University of Alicante, PO Box 99, E-03080, Alicante, Spain
[c] Department of Ecology, University of Alicante, PO Box 99, E-03080, Alicante, Spain
[d] Multidisciplinary Institute for Environmental Studies (MIES), Universidad de Alicante, P.O. Box 99, E-03080, Alicante, Spain

ARTICLE INFO

Article history:
Received 16 July 2019
Received in revised form
15 December 2019
Accepted 16 December 2019
Available online 19 December 2019

Keywords:
Plastic degradation
Biobased and biodegradable plastics
Fourier transform infrared spectroscopy
Differential scanning calorimetry
Marine ecosystems

ABSTRACT

The perdurability of plastics in the environment is one of the major concerns of plastic pollution and, as a consequence, oceans are accumulating large amounts of plastic. The degradation of conventional and biobased materials was evaluated through a laboratory experiment for a year simulating four different conditions in the marine environment. The water column environmental compartment was simulated under euphotic and aphotic (with and without light availability) conditions. The seafloor environmental compartment was simulated with sediment under non-polluted and polluted conditions. By combining weight loss (%), spectroscopic and thermal analyses, the degradation patterns regarding the polymer structure were assessed. The studied biobased materials were polylactic acid (PLA) based materials and showed higher degradability than conventional ones. The weight loss of conventional materials was not influenced by the water column or sediment, while in PLA-based materials, the degradation rates were *ca.* 5 times greater in the sediment than in the water column. The absorbance (Abs) value at 3400 cm^{-1} for polyethylene terephthalate (PET), and carbonyl (CO) index for PET and PLA could be useful to detect early signs of degradation. The crystallization index could be a useful parameter to discriminate degradation stages. The obtained results highlight the different degradability rates of materials depending on the specific environmental marine conditions.

1. Introduction

Plastic pollution is becoming a major environmental threat due to the poor waste management of these types of polymers along with their large perdurability in the environment. Currently, more than 79% of the total plastic production is waste that is not adequately managed, being disposed in landfill or in the environment (Geyer et al., 2017). Marine ecosystems are accumulating large amounts of plastic wastes, receiving every year 4.8–12.7 tones (Jambeck et al., 2015).

Packaging is one of the main uses of single-use plastics, the ones which generate most of the plastic pollution due to the huge production and its short life use making them susceptible to end up in the ocean environment (Andrady, 2011). This situation has led to the development of biodegradable polymers, mainly coming from plant derivatives (Babu Padamati et al., 2013). Polylactic acid (PLA) is one of the major biobased and biodegrable plastic available in the market used mainly as packaging material (Narancic et al., 2018).

In this sense, biodegradable plastics are especially interesting for nondurable applications. These types of plastics allow us to limit their perdurability in the environment and, thus the impact, of this waste when it is not appropriately managed. The main mechanisms of plastic degradation in the environment are photodegradation, thermo-oxidative degradation, hydrolytic degradation and biodegradation by microorganisms (Andrady, 2011). The importance of these mechanisms varies according to the environmental conditions, being, for example, photodegradation significantly decreased in seawater due to low temperature and oxygen levels (Webb et al., 2013). Some studies have evaluated the degradation of PLA and its composites in different environments such as soil (Adhikari et al., 2016), compost (Mihai et al., 2014) and marine

☆ This paper has been recommended for acceptance by Eddy Y. Zeng.

* Corresponding author.
E-mail address: ana.beltran@ua.es (A. Beltrán-Sanahuja).

https://doi.org/10.1016/j.envpol.2019.113836
0269-7491/

conditions (Karamanlioglu et al., 2017) being this process affected by the material properties such as molecular weight and crystallinity and by environmental factors such as temperature, pH, UV light, humidity and the presence of enzymes and microorganisms. In a compost environment, PLA can be degraded by microorganisms after 45–60 days at 50–60 °C (Tokiwa and Calabia, 2006) being the PLA degradation in soil slower than in compost due to the high moisture content present in compost (Itävaara et al., 2002). Regarding aquatic environments, the degradation of PLA samples in seawater was studied by Le Duigou et al. reporting a little change in molecular weight (Le Duigou et al., 2009)

To monitor and evaluate the degradation process of plastic materials, several analytical techniques have been reported in different works. Infrared (IR) spectroscopy has proved to be suitable for the qualitative and quantitative analysis of polymer degradation because it is reliable, fast and cost-effective (Manfredi et al., 2017). In particular, the attenuated total reflectance Fourier transform infrared spectroscopy (ATR-FTIR) is especially useful to monitor changes in the plastic surface due to degradation (Ter Halle et al., 2017). Differential scanning calorimetry (DSC) could also be a good technique to monitor degradability since it determines the thermal properties of plastics, such as melting temperatures and enthalpies, and crystallinity (Andrady, 2017).

To the best of our knowledge only TUV Austria has a certification for marine biodegradability of plastics. However, this certification is focused on the water column on very specific conditions. So, it is needed to develop new methodologies such as the ones presented in this work based on ATR-FTIR, DSC and weight loss analysis to evaluate the plastics degradation in different marine conditions.

The marine environment comprises a wide variety of habitats with markedly different environmental conditions. In the seafloor, sediments are relevant areas of organic matter cycling with large concentrations of microorganisms compared to the water column and, thus the degradation of polymers is expected to be different (Middelburg et al., 1996). In the water column, polymers that are located close to the surface will receive light, favoring photodegradation compared to those present in deep (Copinet et al., 2004). Many marine areas are not only affected by plastic pollution but by other environmental stressors caused by anthropogenic activities. Organic pollution is among the most common types of pollution in the marine environment (Islam and Tanaka, 2004). The extra accumulation of organic matter leads to changes in the reduction-oxidation conditions of the sediment thus modifying the metabolic pathways of degradation of organic matter by microorganisms (Sanz-Lazaro et al., 2011a). Accordingly, all these issues need to be studied to help in the harmonization of standards for marine degradation of polymers.

The aim of this work is to study the degradation of conventional and PLA-based materials through a laboratory experiment embracing different environmental marine conditions for a year. By combining ATR-FTIR, weight loss and DSC analysis, the degradation patterns regarding the polymer structure at both molecular and microscopic levels were assessed.

2. Materials and methods

2.1. Experimental set up

Marine conditions were simulated through a laboratory experiment under controlled conditions using cylinders made of poly (methyl methacrylate) (PMMA) with internal diameter of 5.4 cm and length of 32 or 18 cm, depending on whether it was simulating the seafloor or water column environmental compartments, respectively. Cylinders simulating the seafloor were filled with sediment to a depth of 20 cm. The sediment used was from Mediterranean beach (38°11′018.81″ N 0°35′034.55″ W) and was sieved through a 0.5 mm mesh to remove the large particles and the macrofauna. The sediment was graded as a very fine sand grain (0.063–0.25 mm) according to the Wentworth (1922) classification. All cylinders were filled with filter seawater (filter pore size: 0.5 mm) with a salinity of 37.6 psu. The seawater was oxygenated by air pumps in each cylinder. The cylinders were closed at the bottom with rubber stoppers and the ones with sediment were left to naturally stratify for 10 days before beginning the experiment. Water was changed weekly. Cylinders were maintained at 16 °C by means of two coolers that recirculated the seawater in a tank. The seawater did not exceed the level of the cylinders so there were not transfers among them.

2.2. Reference materials

Four different commercial plastic materials were selected for this study. They included: a multilayer material −polyamide (PA)/polypropylene (PP)-Ethylene-Vinyl-Alcohol (EVOH)-PP - presenting a melting temperature (T_m) of 214 °C, an enthalpy of fusion (ΔH_m) of 8.73 J/g and a crystallization index (CI) of 3.8% for the PA side, and a T_m of 185 °C, an ΔH_m of 5.5 J/g and a CI of 3.9% for the PP side (referenced as A). In this material, the PA used was a PA6 grade polyamide with a melt flow index (MFI) of 130 g/10 min (Temperature: 275 °C, Load: 5.00 Kg). In addition, an EVOH barrier resin film grade with an ethylene content of 32 mol% and low oxygen transmission rate (OTR (cm^3/m^2 day atm; 20 °C; 65%HR; ISO 14663-2) = 0.4) was incorporated as a functional gas and flavour/aroma barrier. Material B was made of polyethylene terephthalate (PET)/polyethylene (PE) presenting a T_m of 117 °C, an ΔH_m of 64. 67 J/g and a CI of 22.3% for the PE side, and a T_m of 245 °C, an ΔH_m of 4. 42 J/g and a CI of 3.3% for the PET side. The material C was a transparent heat-sealable compostable film based on a mixture of polylactic acid (PLA) Ingeo from Natureworks [MFI = 8 g/10 min (Temperature: 210 °C, Load: 2.16 Kg) and 0.4% mol D-Lactide] and cellulose from renewable wood pulp 100% compostable (ASTM D6400, EN13432). On the other hand, the material D was a bilayer of laminate paper/PLA presenting a T_m of 174 °C, ΔH_m of 11.75 J/g and a CI of 12.5%. The PLA used in material D was Ingeo from Natureworks with a number average molecular weight (Mn) of 217000 Da and 2.5%wt D-isomer.

Each material was cut in samples that were rectangles of 3.5 per 1.5 cm. Afterwards, samples were weighed and put inside of fiberglass net bags with a 1 mm mesh size to prevent losses of material. The bags were closed by cotton thread.

2.3. Experimental design

The degradation of materials was tested under four different conditions. In this study, degradation term is used in the broad sense, including also disintegration, since weight loss was included among the parameters used to assess degradation. Regarding the water column environmental compartment, the euphotic zone, the shallow stratum which the sunlight availability is the high (WL); and the aphotic zone, a deep stratum where sunlight is totally attenuated (WD) were simulated. The seafloor environmental compartment was simulated producing two conditions: non-polluted sediment (S) and sediment affected by organic pollution (enrichment) (PS).

In the cylinders simulating the water column conditions, bags were submerged in seawater through glass spheres linked to the bag by a cotton thread. In the cylinders simulating the sediment conditions, bags were buried in the upper stratum (first 4 cm) of the sediment. WL conditions aimed to simulate the light (wavelength and intensity) that it is received in the first 10 m of the water

column and the varying gradually light intensity during the day by means of a Micmol Aqua Air 300 (Micmol, Shenzhen, China). Cylinders under WD conditions were kept in darkness. Organic pollution was simulated in half of the cylinders containing sediment, by enriching fortnightly the surface of the sediment with 0.2 mmol total organic carbon (TOC) cm^{-3} sediment of labile organic matter as a finely ground fish feed [L-4 Alternate CMX 20 2 P BB2, SKRETTING (46.5% protein, 20% fats and oils, 6.1% minerals, 2.2% fibre, 1% phosphorus, 0.9% calcium and 0.4% sodium)]. This amount has demonstrated stimulate the sediment metabolism (Casado-Coy et al., 2017) and represents a possible level of organic pollution in Mediterranean fish farms (Sanz-Lázaro et al., 2011b). Cylinders contained either conventional (A and B) or PLA-based (C and D) materials. Four bags for each material were used per cylinder. Since the degradation of PLA-based materials was expected to be especially high in the sediment, an extra set of cylinders for PLA-based materials was added. Thus, the degradation of all materials under all conditions were tested the days 0, 28, 127, 252 and 365; but for the materials C and D under sediment conditions (S and PS) that were additionally tested for days 51, 70, 87 and 105. Four replicated cylinders were used per condition (WL, WD, S and PS) and per group of materials (conventional or PLA-based), summing up a total of 48 cylinders. Accordingly, on each testing day, two bags (each one corresponding to a different material) were extracted on each cylinder, being 4 replicated measures analyzed for each condition and material.

2.4. Sample pre-treatment

Prior to the analysis, samples were dried for 24 h in an oven at 30 °C. Afterwards, samples were washed twice in distilled water for 5 min and kept in a desiccator shielded from light. Analysis of the samples was carried out in order to monitor the weight loss and to ascertain any potential modifications as identified through ATR-FTIR and DSC analysis.

2.5. Weight loss analysis

The weight loss of each material was calculated by weight difference between day 0 and the corresponding testing day:

$$\%\ \text{weight loss: } [(m_o - m_t)/m_o]x100$$

where m_o is the initial mass of the material (day 0) and m_t is the mass at the extraction point at time t in grams. Each material was weighed using a precision balance (±0.0001 g).

2.6. Fourier transform infrared (FTIR) spectroscopy

Infrared spectra were recorded using a Bruker Analitik IFS 66 FTIR spectrometer (Ettlingen, Germany) equipped with a DTGS KBr detector and a Golden Gate Single Reflection Diamond ATR accessory (incident angle of 45°). Spectra were recorded in the absorbance mode from 4.000 to 600 cm^{-1}; using 64 scans and 4 cm^{-1} resolution and corrected against the background spectrum of air. Two spectra replicates were obtained for each sample. In relation to material A, the degradation was evaluated by the calculation of the PA index defined as the area of the absorption band assigned to the N–H bend, C–N stretch relative to the area of the amide C=O stretching absorption band. The amide C=O absorption band was considered in the 1585-1800 cm^{-1} region and the N–H bend, C–N stretch absorption band was taken in the 1490-1585 cm^{-1} region. Regarding the material B, the maximum value of absorbance of the band in the hydroxyl region (3200–3500 cm^{-1}) of PET spectra was evaluated following the aging treatment since this band has been tentatively ascribed to the –OH stretching vibration of newly formed carboxylic acid end groups (Arrieta et al., 2013). In addition, the degradation was evaluated by the calculation of the CO index defined as the area of the absorbance of the carbonyl group (C=O) absorption band relative to the area of the absorbance of the C–O stretching band. The C=O absorption band was considered in the 1600-1780 cm^{-1} region and the C–O stretch absorption band was taken in the 1030-1160 cm^{-1} region. In relation to materials C and D, the degradation was also evaluated by the calculation of the CO index. In these materials, the C=O absorption band was considered in the 1600-1830 cm^{-1} region and the C–O stretch absorption band was taken in the 950-1340 cm^{-1} region.

2.7. Differential scanning calorimetry (DSC)

Thermal characterizations were performed with a TA DSC Q-100 (New Castle, DE, USA) equipment under nitrogen atmosphere. Samples were introduced in aluminum pans (40 μL). They were heated from ambient temperature to 250 °C, 300 °C or 200 °C, depending on whether they were samples of material A, B or D, respectively. Afterwards, samples were cooled to −90 °C and finally heated again to 250 °C, 300 °C or 200 °C, (heating/cooling speed = 10 °C/min). Calorimetric curves were analyzed using the Universal Analysis TM Software (TA Instruments, New Castle) to obtain enthalpy (ΔH, J/g), calculated from the area under the DSC curves, and peak temperature values (°C) corresponding to the maximum of the observed transitions. The crystallization and melting parameters were determined from the first heating event.

The CI was calculated using the expression (Valdés et al., 2016):

$$CI = \Delta H_m/(\Delta H^\circ_m)x100$$

where ΔH_m is the melting enthalpy per unit mass of the sample and ΔH°_m the theoretical value of the melting enthalpy per unit mass of 100% crystalline PE (290 J/g), PP (138 J/g), PET (135.8 J/g), PA (230 J/g) and PLA (93.7 J/g) (Davachi and Kaffashi, 2015).

2.8. Statistical analysis

The trends of the loss of weight of each material on each simulated environmental condition were modelled through time. The model was chosen by adjusting the data to the best fitted regression models using the Akaike information criterion. Then, the trends among the simulated environmental conditions were compared through analysis of covariance (ANCOVA). Statistical analyses were performed with R statistical software (v. 2.15.0) using the packages “AICcmodavg”, “plyr” and “stringr”. All data were reported as mean ± standard error (SE). Statistical tests were conducted with a significance level of $\alpha = 0.05$ (Underwood, 1997).

3. Results and discussion

3.1. Weight loss analysis

Under conditions simulating the water column, the weight of conventional materials remained stable during the whole experiment, especially in the case of material B in the water column under dark conditions (Fig. 1). The material B under light conditions and material A in both conditions showed a slight tendency of weight loss reaching a value of 0.5% approximately after 365 days. Nevertheless, there was not a significant different trend of weight loss along time among the conventional materials disregarding the light conditions (Table 1). In the case of PLA-based materials, the weight loss was much more noticeable, especially in material C (Table 1) reaching a value of 29.2% weight loss in WL and a value of 24.6%

weight loss in WD (Fig. 1). In relation to material D, the values of weight loss were 5.6 and 6.0% in WL and WD respectively.

Under conditions simulating the seafloor, a similar trend was found for conventional materials, being in this case material B under organic pollution the material that remained more stable along time in terms of weight loss, while the material B under non pollution conditions and material A in both conditions showed a slight tendency of weight loss reaching a value of 0.9% approximately after 365 days. There was not a significant different trend in weight loss along time among the conventional materials regardless the pollution conditions (Table 1). PLA-based materials showed a significantly different trend compared to conventional ones. In both materials, the absence of pollution favored degradation (Table 1, Fig. 1). Material C under conditions of no pollution showed total degradation after 128 days, while material D reached a value of 75.3% weight loss after 365 days.

The weight loss of conventional materials was not influenced by the environmental compartment (water column or seafloor), while in the case of PLA-based materials, the degradation rates were *ca.* 5 times greater in the sediment than in the water column (Fig. 1). Marine sediments are one of the largest areas of organic matter mineralization (Middelburg et al., 1993), since they harbour large numbers of bacteria compared to the water column (Accinelli et al., 2012). Thus, the seafloor is expected to be an environment that favours plastic degradation (Thellen et al., 2008) and our results are in agreement with this rationale.

The low degradability of the studied conventional materials could be explained due to the high hydrophobic level and high molecular weight of polyolefins, such as PE and PP (Fotopoulou and Karapanagioti, 2017). In relation to aromatic polyesters such as PET this polymer is considered resistant to environmental and biological agents (Eubeler et al., 2010) as it can be concluded from the weight loss results obtained in this study for material B. On the other hand, as a polymer synthesized by condensation, polyamide (PA) is likely to undergo chemical attack from water in the presence of moisture, as the amide bond is especially susceptible to both acid and base-catalyzed hydrolysis. Photodegradation of aliphatic polyamides is characterized by the cleavage of the –N-C- bond at

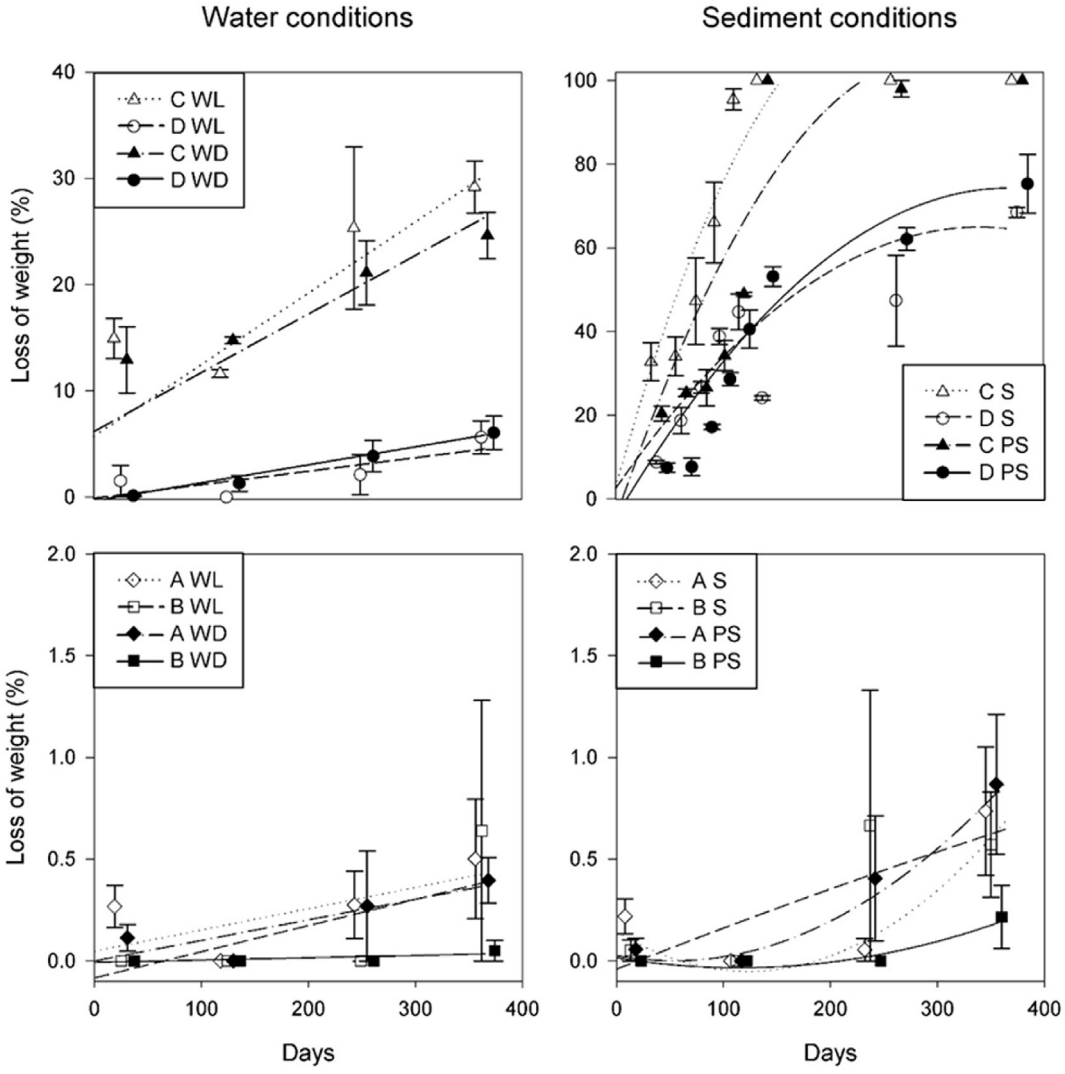

Fig. 1. Trends of weight loss (mean ± SE, n = 4) of the different materials on the different simulated conditions. The first letter refers to the material. "WL" and "WD" stand for euphotic (with light) and aphotic (without light) conditions, respectively. "S" and "PS" stand for non-polluted and polluted sediment, respectively. Despite being measured at the same days, conditions are slightly displaced from the time in the plot to avoid overlapping and facilitate visualization. When the regression reached a level of weight loss of 100% the rest of the regression was not represented to avoid misinterpretation. In the case of the water column and sediment, a regression model was done for all conditions replicated for all materials, in the water column and in the sediment, respectively. The R^2 values of the regressions were 0.85 and 0.93, respectively, being in both cases significant ($p < 0.001$). Coefficients of the regressions are shown in Table 1.

Table 1
Coefficients (mean ± SE, n = 4) of the first- ($y_i = \beta_0 + \beta_1 x_i$) and second-order ($y_i = \beta_0 + \beta_1 x_i + \beta_2 x_i^2$) polynomial regression models showing the loss of weight of the different materials along time within the different conditions. Significant effects ($p < 0.05$) are indicated in bold. Baselines are material A, and euphotic and no pollution conditions, for water column and sediment conditions, respectively.

Conditions			β_0	β_1	β_2
Water column	Euphotic	Material A	0.09 ± 1.4	0.0009 ± 0.01	–
		Material B	−0.24 ± 2.1	0.0006 ± 0.009	–
		Material C	**10.3 ± 2**	**0.049 ± 0.009**	–
		Material D	−0.3 ± 2	0.012 ± 0.009	–
	Aphotic	Material A	−0.09 ± 2	0.0001 ± 0.009	–
		Material B	0.23 ± 2.9	−0.0015 ± 0.013	–
		Material C	0.93 ± 2.9	−0.014 ± 0.013	–
		Material D	−0.36 ± 2.9	0.0049 ± 0.012	–
Sediment	No pollution	Material A	0.14 ± 3.8	−0.003 ± 5.9	0.00001 ± 1.6
		Material B	−0.18 ± 5.3	0.005 ± 8.4	−0.00001 ± 2.3
		Material C	2.8 ± 5.1	**0.91 ± 8.0**	**−0.002 ± 2.1**
		Material D	2.4 ± 5.2	**0.37 ± 8.5**	**−0.0006 ± 2.3**
	Pollution	Material A	−0.12 ± 5.3	0.002 ± 8.5	−0.000004 ± 2.3
		Material B	0.2 ± 7.5	−0.005 ± 1.2	0.00001 ± 3.2
		Material C	−7.45 ± 7.2	−0.17 ± 1.2	0.001 ± 3.1
		Material D	−6.75 ± 7.3	0.06 ± 1.2	−0.00004 ± 3.2

short light radiation wavelengths (254 nm) to produce amine and aldehyde groups (Arrieta et al., 2013). In relation to PA, the mass of the material also remains constant throughout the four different degradation treatments, so it is possible to assume that a lower density brought about by the lower crystalline fraction found in aged PA material would be the most likely phenomenon to account for the obtained results (Arrieta et al., 2013).

In contrast, the weight loss (%) values obtained for PLA-based materials were higher than the ones obtained for conventional ones as it was expected (Emadian et al., 2017).

3.2. ATR-FTIR analysis

Material A did not showed new absorption bands in the FTIR spectra of PA under any tested marine condition (Table 2). As it has been reported by other authors, photodegradation of PA is expected to result in the formation of aldehydic and acidic groups, whereas carboxylic acid and amine groups are the final products of the hydrolysis reaction (Arrieta et al., 2013). Both aldehydes and acid groups display a strong absorption band in the carbonyl region corresponding to the C=O stretching vibration that makes IR band assignment a relatively straightforward procedure.

However, since the FTIR spectra of virgin PA already exhibits strong bands in the carbonyl region, any new band in this region linked to the formation of chemical degradation products could not be detected due to overlapping with the existing bands. For this reason, no significant differences were observed regarding PA index (material A) among any of the simulated environmental conditions

Table 2
PA index of material A, CO index and absorbance value at 3400 cm^{-1} of material B and CO index for materials C and D at different days under the four marine conditions. FTIR parameters are expressed as average quantities ± standard deviation of four replicates for each sample (n = 4). "WL" and "WD" stand for euphotic (with light) and aphotic (without light) conditions, respectively. "S" and "PS" stand for non-polluted and polluted sediment conditions, respectively. nm: not measured.

Conditions	Days	Material A	Material B		Material C	Material D
		PA	PET		PLA	PLA
		PA index	CO index	Abs 3400 cm^{-1}	CO index	CO index
	0	0.79 ± 0.01	0.86 ± 0.04	0.04 ± 0.01	0.54 ± 0.02	0.03 ± 0.00
PS	**28**	0.74 ± 0.01	0.90 ± 0.10	0.04 ± 0.01	0.53 ± 0.01	0.03 ± 0.00
	51	nm	nm	nm	0.52 ± 0.01	0.44 ± 0.03
	70	nm	nm	nm	0.54 ± 0.01	0.47 ± 0.03
	87	nm	nm	nm	0.52 ± 0.01	0.32 ± 0.21
	105	nm	nm	nm	0.50 ± 0.01	0.40 ± 0.06
	127	0.76 ± 0.02	0.93 ± 0.09	0.05 ± 0.01	0.79 ± 0.23	0.37 ± 0.16
	252	0.73 ± 0.06	1.18 ± 0.05	0.09 ± 0.00	nm	0.49 ± 0.08
	365	0.76 ± 0.07	1.26 ± 0.08	0.14 ± 0.02	nm	0.91 ± 0.09
S	**28**	0.75 ± 0.01	0.95 ± 0.06	0.03 ± 0.00	0.54 ± 0.00	0.03 ± 0.00
	51	nm	nm	nm	0.53 ± 0.01	0.42 ± 0.02
	70	nm	nm	nm	0.52 ± 0.02	0.45 ± 0.02
	87	nm	nm	nm	0.46 ± 0.08	0.34 ± 0.22
	105	nm	nm	nm	0.50 ± 0.06	0.39 ± 0.18
	127	0.81 ± 0.04	0.82 ± 0.12	0.05 ± 0.02	0.53 ± 0.04	0.43 ± 0.09
	252	0.76 ± 0.02	1.11 ± 0.16	0.10 ± 0.00	nm	0.44 ± 0.01
	365	0.75 ± 0.02	1.05 ± 0.09	0.15 ± 0.02	nm	0.85 ± 0.03
WL	**28**	0.75 ± 0.01	0.94 ± 0.08	0.04 ± 0.01	0.52 ± 0.02	0.03 ± 0.01
	127	0.75 ± 0.01	0.93 ± 0.10	0.06 ± 0.01	0.53 ± 0.02	0.41 ± 0.16
	252	0.75 ± 0.04	0.86 ± 0.08	0.05 ± 0.01	0.55 ± 0.06	0.39 ± 0.02
	365	0.75 ± 0.04	0.92 ± 0.08	0.05 ± 0.00	0.54 ± 0.06	0.72 ± 0.05
WD	**28**	0.78 ± 0.02	0.90 ± 0.09	0.04 ± 0.01	0.52 ± 0.01	0.02 ± 0.02
	127	0.76 ± 0.01	0.91 ± 0.09	0.05 ± 0.00	0.55 ± 0.05	0.40 ± 0.05
	252	0.73 ± 0.03	1.05 ± 0.20	0.04 ± 0.00	0.54 ± 0.03	0.42 ± 0.05
	365	0.76 ± 0.04	1.01 ± 0.10	0.05 ± 0.00	0.55 ± 0.03	0.75 ± 0.06

Table 3
Melting temperature (T_m, °C), melting enthalpy (ΔH_m, J/g) and crystallization index (CI) of the studied materials at different days of the four degradation treatments. DSC parameters are expressed as average quantities ± standard deviation of four replicates for each sample (n = 4). "WL" and "WD" stand for euphotic (with light) and aphotic (without light) conditions, respectively. "S" and "PS" stand for non-polluted and polluted sediment conditions, respectively. nm: not measured.

Treatment	Days	Material A						Material B						Material D		
		PP			PA			PE			PET					
		T_m	ΔH_m	CI	T_m	ΔH_m	CI	T_m	ΔH_m	CI	T_m	ΔH_m	CI	T_m	ΔH_m	CI
PS	**0**	180 ± 0	5.5 ± 0.7	4.0 ± 0.5	214 ± 1	11.7 ± 0.5	5.1 ± 0.2	111 ± 1	64.7 ± 1.3	22.3 ± 0.4	245 ± 1	7.4 ± 0.5	5.5 ± 0.4	174 ± 0	11.7 ± 1.4	13.4 ± 0.9
	28	180 ± 0	5.5 ± 0.2	4.1 ± 0.1	212 ± 2	11.8 ± 0.8	5.1 ± 0.4	111 ± 1	64.5 ± 0.6	21.1 ± 0.4	245 ± 1	7.5 ± 0.4	5.6 ± 0.3	173 ± 1	12.7 ± 1.1	13.6 ± 1.2
	51	nm	nm	nm	nm	nm	nm	nm	nm	nm	nm	nm	nm	174 ± 0	12.5 ± 0.9	13.4 ± 0.9
	70	nm	nm	nm	nm	nm	nm	nm	nm	nm	nm	nm	nm	174 ± 1	12 .3 ± 1.1	13.1 ± 1.2
	87	nm	nm	nm	nm	nm	nm	nm	nm	nm	nm	nm	nm	174 ± 0	13.5 ± 0.6	14.4 ± 0.6
	105	nm	nm	nm	nm	nm	nm	nm	nm	nm	nm	nm	nm	174 ± 1	16.8 ± 0.7	17.9 ± 0.8
	127	180 ± 0	5.4 ± 0.1	3.9 ± 0.1	212 ± 1	10.6 ± 0.4	4.6 ± 0.2	110 ± 1	64.3 ± 1.4	22.1 ± 0.5	245 ± 1	6.5 ± 0.4	4.7 ± 0.3	174 ± 0	18.7 ± 1.2	20.1 ± 1.6
	252	180 ± 0	4.1 ± 0.6 2.9 ± 0.5	2.9 ± 0.5	212 ± 1	8.8 ± 1.4	3.8 ± 0.6	110 ± 1	62.6 ± 0.5	21.5 ± 0.2	245 ± 1	5.9 ± 0.4	4.4 ± 0.3	173 ± 1	30.8 ± 4.7	32.8 ± 5.1
	365	180 ± 1	3.8 ± 0.4	2.8 ± 0.3	212 ± 1	7.6 ± 0.9	3.3 ± 0.4	110 ± 1	60.4 ± 0.8	20.8 ± 0.5	245 ± 1	4.8 ± 0.4	3.5 ± 0.3	174 ± 1	37.2 ± 1.9	39.5 ± 2.1
S	**28**	179 ± 1	6.5 ± 1.7	4.7 + 1.3	211 ± 2	11.3 ± 0.3	4.9 ± 0.1	110 ± 1	63.5 ± 2.1	21.9 ± 0.7	244 ± 1	7.5 ± 0.4	5.5 ± 0.3	174 ± 1	12.5 ± 0.4	13.3 ± 0.5
	51	nm	nm	nm	nm	nm	nm	nm	nm	nm	nm	nm	nm	174 ± 0	13.9 ± 1.5	14.8 ± 1.6
	70	nm	nm	nm	nm	nm	nm	nm	nm	nm	nm	nm	nm	174 ± 0	13.5 ± 0.2	14.4 ± 0.2
	87	nm	nm	nm	nm	nm	nm	nm	nm	nm	nm	nm	nm	174 ± 0	13.9 ± 0.8	14.8 ± 0.9
	105	nm	nm	nm	nm	nm	nm	nm	nm	nm	nm	nm	nm	174 ± 1	14.8 ± 0.7	15.8 ± 0.7
	127	180 ± 0	5.1 ± 0.6	3.7 ± 0.4	209 ± 4	9.7 ± 1.8	*42* ± 0.8	110 ± 1	64.4 ± 0.8	22.2 ± 0.3	245 ± 1	6.3 ± 0.S	4.6 ± 0.6	174 ± 0	15.7 ± 0.2	16.7 ± 2.2
	252	180 ± 0	4.2 ± 0.2	3.1 ± 0.2	213 ± 0	9.1 ± 0.5	4.0 ± 0.2	110 ± 1	63.9 ± *12*	22.1 ± 0.4	245 ± 1	5.6 ± 0.3	4.1 ± 0.2	174 ± 0	19.3 ± 3.9	24.4 ± 2.0
	365	180 ± 1	4.0 ± 0.1	2.9 ± 0.1	212 ± 1	8.6 ± 0.8	3.7 ± 0.3	110 ± 1	61.5 ± 0.5	21.2 ± 0.2	245 ± 1	4.6 ± 0.4	3.4 ± 0.3	174 ± 1	21.8 ± 1.5	24.4 ± 2.0
WL	**28**	180 ± 0	5.2 ± 0.4	3.8 ± 0.3	209 ± 1	10.5 ± 0.1	4.6 ± 0.1	111 ± 1	66.1 ± 2.2	19.3 ± 0.7	245 ± 1	6.7 ± 0.7	4.9 ± 0.5	170 ± 1	10.4 ± 0.9	11.1 ± 1.1
	127	180 ± 0	5.3 ± 0.3	3.8 ± 0.3	210 ± 2	10.4 ± 0.5	4.5 ± 0.2	110 ± 1	61.8 ± 2.8	21.3 ± 0.9	245 ± 1	5.9 ± 0.1	4.4 ± 0.1	170 ± 0	11.2 ± 0.6	11.9 ± 0.9
	252	180 ± 0	4.1 ± 0.2	3.0 ± 0.1	211 ± 2	9.2 ± 0.6	4.1 ± 0.2	110 ± 1	62.0 ± 2.8	21.4 ± 0.9	244 ± 1	5.8 ± 0.5	4.3 ± 0.4	171 ± 0	10.2 ± 0.8	10.9 ± 0.8
	365	180 ± 1	4.0 ± 0.3	2.9 ± 0.2	212 ± 1	9.1 ± 0.2	3.9 ± 0.1	110 ± 0	61.7 ± 0.7	21.1 ± 0.5	245 ± 0	5.6 ± 0.7	4.2 ± 0.3	174 ± 1	10.5 ± 0.3	11.2 ± 0.4
WD	**28**	180 ± 0	5.4 ± 0.2	3.9 ± 0.1	211 ± 2	10.6 ± 0.3	4.6 ± 0.1	111 ± 1	63.1 ± 1.7	18.3 ± 0.6	245 ± 1	6.8 ± 0.6	5.1 ± 0.4	174 ± 1	10.9 ± 0.3	11.6 ± 0.3
	127	180 ± 0	5.4 ± 0.1	3.9 ± 0.1	213 ± 1	10.3 ± 0.1	4.5 ± 0.1	110 ± 1	62.5 ± 2.3	21.5 ± 0.8	245 ± 1	6.5 ± 0.3	4.8 ± 0.3	174 ± 0	11.8 ± 0.9	12.7 ± 1.0
	252	180 ± 1	3.9 ± 0.5	2.8 ± 0.4	210 ± 2	8.7 ± 0.4	3.8 ± 0.2	111 ± 1	60.6 ± 1.6	20.9 ± 0.5	244 ± 1	5.9 ± 0.2	4.3 ± 0.2	173 ± 1	10.4 ± 0.9	11.1 ± 0.9
	365	180 ± 1	3.8 ± 0.2	2.7 ± 0.2	212 ± 0	8.5 ± 0.4	3.7 ± 0.2	110 ± 0	60.4 ± 0.7	20.7 ± 0.5	245 ± 0	5.8 ± 0.5	4.3 ± 0.2	173 ± 2	10.0 ± 0.8	11.0 ± 0.9

at any time. Despite so, the material could have already suffered to some extent degradation due to weathering although it could not be noticed by FTIR.

In relation to material B, the analysis of the hydroxyl band present in FTIR spectra of PET indicates the formation of a new absorption band towards 3400 cm^{-1} related to degradation. This band has been tentatively ascribed to the −OH stretching vibration of newly formed carboxylic acid end groups, which are believed to be the product of chemical degradation reactions. The development of this band is consistent with previous works on the chemical degradation of PET (Arrieta et al., 2013) and the formation is more pronounced in samples in marine sediments compared to samples in the water column. This fact again indicates that sediments could have a favourable effect on degradation (Eubeler et al., 2010) being in accordance with the results obtained in this work for weight loss (%). In addition, for PET material, the absorbance of the band at 3400 cm^{-1} is directly related to the CO index value since the index is depending on the absorbance of the carbonyl group band and the absorbance of the C—O stretching band. Since the formation of newly acid end groups in the material as the degradation occurs implies the formation of new carbonyl bonds, it is expected that the value of the CO index will also increase as the degradation progresses, a fact that is confirmed by the data presented in Table 2, being the increase more accused in samples in marine sediment as it was expected.

The degradation of PLA in a simulated marine environment is based on a hydrolysis reaction which is usual for polyesters. As it has been reported by other authors (Pelegrini et al., 2015), the hydrolytic degradation mechanism occurs by diffusion of water toward the polymer interior, promoting scission of ester linkages, reducing chains into soluble fragments, and leading to lower molar mass. Finally, the by-product formed in the PLA hydrolytic degradation process is lactic acid, which is subsequently incorporated into cycles of carboxylic acids, carbon dioxide, and water. As a consequence of the degradation process, the CO index of materials C and D increases since the formation of acid groups of lactic acid involves the formation of carbonyl bonds. Regarding the material C, only a slight increase in this value is observed in samples in organic polluted marine sediments after 127 days. After that, samples of days 252 and 365 could not be measured because this material was totally degraded and no samples were found to evaluate their degradation by using FTIR.

Concerning the degradation of material D, a significant increase in the CO index was observed under all conditions as the degradation of the material occurs. In this sense, the increase was more pronounced in samples simulating marine sediments in comparison with samples in the water column. For detailed explanations on the ATR-FTIR analysis of the virgin materials, see Supporting Information.

3.3. DSC analysis

Crystallization index (CI) and melting parameters (temperatures and enthalpies) were calculated from DSC curves for all material samples under the four different degradation treatments at different days as it is shown in Table 3. Values obtained for the repeatability of the process were dependent on the selected parameter with relative standard deviations lower than 1% for melting temperature (T_m) in all cases and a mean value of 10% for CI and ΔH_m. The melting temperature of PE, PP, PA, PET and PLA remained unaffected during the whole experiment under all tested marine conditions showing that this parameter is not affected by aging, which agrees with previous studies (Copinet et al., 2004; Webb et al., 2013). On the other hand, changes in the melting enthalpy [ΔH_m (J/g)] and CI may indicate degradation of the materials. In this sense, plastics such as PE, PP, PA, PET and PLA are semi-crystalline materials that are made up of micro-scale hard crystallites embedded in a soft amorphous matrix. An increase in the CI can occur when the amorphous zones of the polymer are preferentially degraded increasing fractional crystallinity as it occurred in PLA-based samples in the seafloor environmental compartment irrespectively of the existence of pollution. A possible explanation for an increase of crystallinity is that the amorphous chains acquire increased mobility after partial photo-oxidation and chain scission (Copinet et al., 2004). The increase in crystallinity in these samples result in a correspondingly higher density of microplastics rendering them negatively buoyant. This fact determines its location and selects the range of marine organisms the microplastics can interact with (Islam and Tanaka, 2004). However, no significant changes in melting enthalpy and crystallinity were observed in PLA-based samples that were under the water column conditions during the experiment. These results are in accordance with the ones obtained related to weight loss in this work and previous studies that indicate that sediments could have a favourable effect on degradation since they harbour higher microbial densities than other environments such as the water column (Middelburg et al., 1993; Eubeler et al., 2010). The higher values of CI obtained for the material D can be related to higher rates of degradation of the amorphous fraction of the material in comparison with materials A and B as it was expected since the crystalline areas are reported to be the last to be degraded (Perez et al., 2013). The higher values of CI for material D were obtained at 365 days under marine sediment conditions indicating that the sediment is a suitable source for PLA degradation being these results in accordance with other works (Emadian et al., 2017).

However, since the degradation of the polymer occurs mainly in the surface layer, as relatively more crosslinking occurs in later weathering some of the crystallinity might be reduced as we found in the materials A and B. With a gradual incorporation of smaller and defective molecules during degradation, the imperfect recrystallization could reduce the crystallinity (Lv et al., 2015).

4. Conclusions

The degradation of PLA-based materials under simulated marine conditions was much more marked compared to conventional materials. The differential degradation rates of materials were mainly dependent on the environmental compartment: water column or seafloor, and to a lesser extent, to other conditions such as light availability or pollution. The Abs 3400 cm^{-1} for PET and CO index for PET and PLA-based materials and the CI could be useful to detect early signs of degradation even before a notable loss of weight occurs, helping to estimate the degradation time of a waste material found in the environment.

CRediT authorship contribution statement

Ana Beltrán-Sanahuja: Conceptualization, Methodology, Writing - original draft. **Nuria Casado-Coy:** Investigation, Methodology. **Lorena Simó-Cabrera:** Data curation, Formal analysis. **Carlos Sanz-Lázaro:** Conceptualization, Supervision, Writing - review & editing.

Acknowledgements

This work has been funded by the Spanish Foundation for Science and Technology (FECYT2-19I; PR238). C. S. was funded by the University of Alicante (Ref. UATALENTO 17-11). Authors are grateful for the students that helped in the running of the experiments: Laura Tovar, Rocío Huget, Ana Belén Jodar, Amanda Cohen, Susana

Carrión and Lázaro Ruiz.

Appendix A. Supplementary data

Supplementary data to this article can be found online at https://doi.org/10.1016/j.envpol.2019.113836.

References

Accinelli, C., Saccà, M.L., Mencarelli, M., Vicari, A., 2012. Deterioration of bioplastic carrier bags in the environment and assessment of a new recycling alternative. Chemosphere 89, 136–143. https://doi.org/10.1016/j.chemosphere.2012.05.028.

Adhikari, D., Mukai, M., Kubota, K., Kai, T., Kaneko, N., Araki, K.S., Kubo, M., 2016. Degradation of bioplastics in soil and their degradation effects on environmental microorganisms. J. Agric. Chem. Environ. 5, 23–34. https://doi.org/10.4236/jacen.2016.51003.

Andrady, A., 2011. Microplastics in the marine environment. Mar. Pollut. Bull. 62, 1596–1605. https://doi.org/10.1016/j.marpolbul.2011.05.030.

Andrady, A., 2017. The plastic in microplastics: a review. Mar. Pollut. Bull. 11, 12–22. https://doi.org/10.1016/j.marpolbul.2017.01.082.

Arrieta, C., Dong, Y., Lan, A., Vu-Khanh, T., 2013. Outdoor weathering of polyamide and polyester ropes used in fall arrest equipment. J. Appl. Polym. Sci. 130 (5), 3058–3065. https://doi.org/10.1002/app.39524.

Babu Padamati, R., O'Connor, K., Seeram, R., 2013. Current progress on bio-based polymers and their future trends. Prog Biomater 2, 8. https://doi.org/10.1186/2194-0517-2-8.

Copinet, A., Bertrand, C., Govindin, S., Coma, V., Couturier, Y., 2004. Effects of ultraviolet light (315 nm), temperature and relative humidity on the degradation of polylactic acid plastic films. Chemosphere 55 (5), 763–773. https://doi.org/10.1016/j.chemosphere.2003.11.038.

Casado-Coy, N., Martínez-García, E., Sánchez-Jerez, P., Sanz-Lázaro, C., 2017. Mollusc-shell debris can mitigate the deleterious effects of organic pollution on marine sediments. J. Appl. Ecol. 54 (2), 547–556. https://doi.org/10.1111/1365-2664.12748.

Davachi, S.M., Kaffashi, B., 2015. Preparation and characterization of poly L-lactide/triclosan nanoparticles for specific antibacterial and medical applications. Int. J. Polym. Mater. Polym. Biomater. 64, 497–508. https://doi.org/10.1080/00914037.2014.977897.

Emadian, S.M., Onay, T.T., Demirel, B., 2017. Biodegradation of bioplastics in natural environments. Waste Manag. 59, 526–536. https://doi.org/10.1016/j.wasman.2016.10.006.

Eubeler, J.P., Bernhard, M., Knepper, T.P., 2010. Environmental biodegradation of synthetic polymers II. Biodegradation of different polymer groups. Trends Anal. Chem. **29** (1), 84–100. https://doi.org/10.1016/j.trac.2009.09.005.

Fotopoulou, K.N., Karapanagioti, H.K., 2017. Degradation of various plastics in the environment. Hazardous chemicals associated with plastics in the marine environment. In: The Handbook of Environmental Chemistry, vol. 78. Springer, Cham, pp. 71–92.

Geyer, R., Jambeck, J.R., Law, K.L., 2017. Production, use, and fate of all plastics ever made. Sci Adv 3 (7), e1700782. https://doi.org/10.1126/sciadv.1700782.

Islam, M.D., Tanaka, M., 2004. Impacts of pollution on coastal and marine ecosystems including coastal and marine fisheries and approach for management: a review and synthesis. Mar. Pollut. Bull. 48 (7–8), 624–649. https://doi.org/10.1016/j.marpolbul.2003.12.004.

Itävaara, M., Karjomaa, S., Selin, J.-F., 2002. Biodegradation of polylactide in aerobic and anaerobic thermophilic conditions. Chemosphere 46 (6), 879–885. https://doi.org/10.1016/S0045-6535(01)00163-1.

Jambeck, J.R., Geyer, R., Wilcox, C., Siegler, T.R., Perryman, M., Andrady, A., Narayan, R., Law, K.L., 2015. Plastic waste inputs from land into the ocean. Science 347 (6223), 768–771. https://doi.org/10.1126/science.1260352.

Karamanlioglu, M., Preziosi, R., Robson, G.D., et al., 2017. Abiotic and biotic environmental degradation of the bioplastic polymer poly(lactic acid): A review. Polymer Degradation and Stability 137, 122–130. https://doi.org/10.1016/j.polymdegradstab.2017.01.009.

Le Duigou, A., Davies, P., Baley, C., 2009. Seawater ageing of flax/poly(lactic acid) biocomposites. Polym. Degrad. Stab. 94, 1151–1162. https://doi.org/10.1016/j.polymdegradstab.2009.03.025.

Lv, Y., Huang, Y., Yang, J., Kong, M., Yang, H., Zhao, Y., Li, G., 2015. Outdoor and accelerated laboratory weathering of polypropylene: a comparison and correlation study. Polym. Degrad. Stab. 112, 145–159. https://doi.org/10.1016/j.polymdegradstab.2014.12.023.

Manfredi, M., Barberis, E., Marengo, E., 2017. Prediction and classification of the degradation state of plastic materials used in modern and contemporary art. Appl. Phys. A 123, 35. https://doi.org/10.1007/s00339-016-0663-x.

Middelburg, J.J., Vlug, T., Jaco, F., Van der Nat, W.A., 1993. Organic matter mineralization in marine systems. Glob. Planet. Chang. 8 (1–2), 47–58. https://doi.org/10.1016/0921-8181(93)90062-S.

Middelburg, J.J., Soetaert, K., Herman, P., Heip, C., 1996. Denitrification in marine sediments: a model study. Glob. Biogeochem. Cycles 10 (4), 661–673. https://doi.org/10.1029/96GB02562.

Mihai, M., Legros, N., Alemdar, A., 2014. Formulation-properties versatility of wood fiber biocomposites based on polylactide and polylactide/thermoplastic starch blends. Polym. Eng. Sci. 54 (6), 1325–1340. https://doi.org/10.1002/pen.23681.

Narancic, T., Verstichel, S., Chaganti, S.R., Morales-Gamez, L., Kenny, S.T., De Wilde, B., Babu Padamati, R., O'Connor, K.E., 2018. Biodegradable plastic blends create new possibilities for end-of-life management of plastics but they are not a panacea for plastic pollution. Environ. Sci. Technol. 52 (18), 10441–10452. https://doi.org/10.1021/acs.est.8b02963.

Pelegrini, K., Donazzolo, I., Brambilla, V., Coulon Grisa, A.M., Piazza, D., Zattera, A.J., Brandalise, R.N., 2015. Degradation of PLA and PLA in composites with triacetin and buriti fiber after 600 days in a simulated marine environment. J. Appl. Polym. Sci. 133 (15) https://doi.org/10.1002/app.43290.

Perez, C.J., Failla, M.D., Carella, J.M., 2013. SSA study of early polyethylenes degradation stages. Effects of attack rate, of average branch length, and of backbonepolymethylene sequences length distributions. Polym. Degrad. Stab. 98 (1), 177–183. https://doi.org/10.1016/j.polymdegradstab.2012.10.012.

Sanz-Lazaro, C., Valdemarsen, T., Marin, A., Holmer, M., 2011a. Effect of temperature on biogeochemistry of marine organic-enriched systems: implications in a global warming scenario. Ecol. Appl. 21, 2664–2677. https://doi.org/10.1890/10-2219.1.

Sanz-Lázaro, C., Belando, M.D., Marín-Guirao, L., Navarrete-Mier, F., Marín, A., 2011b. Relationship between sedimentation rates and benthic impact on Maërl beds derived from fish farming in the Mediterranean. Mar. Environ. Res. 71 (1), 22–30. https://doi.org/10.1016/j.marenvres.2010.09.005.

Ter Halle, A., Ladirat, L., Martigna, M., Françoise Mingotaud, A., Boyron, O., Perez, E., 2017. To what extent are microplastics from the open ocean weathered? Environ. Pollut. 227, 167–174. https://doi.org/10.1016/j.envpol.2017.04.051.

Thellen, C., Coyne, M., Froio, D., Auerbach, M., Wirsen, C., Ratto, J.A., 2008. A processing, characterization and marine biodegradation study of melt-extruded polyhydroxyalkanoate (PHA) films. J. Polym. Environ. 16, 1–11. https://doi.org/10.1007/s10924-008-0079-6.

Tokiwa, Y., Calabia, B.P., 2006. Biodegradability and biodegradation of poly(lactide). Appl. Microbiol. Biotechnol. 72 (2) https://doi.org/10.1007/s00253-006-0488-1, 244-25.

Underwood, A.J., 1997. Experiments in Ecology: Their Logical Design and Interpretation Using Analysis of Variance. Cambridge University Press, Cambridge.

Valdés, A., Fenollar, O., Beltrán, A., Balart, R., Fortunati, E., Kenny, J.M., Garrigós, M.C., 2016. Characterization and enzymatic degradation study of poly(ε-caprolactone)-based biocomposites from almond agricultural by-products. Polym. Degrad. Stab. 132, 181–190. https://doi.org/10.1016/j.polymdegradstab.2016.02.023.

Webb, H.K., Arnott, J., Crawford, R.J., Ivanova, E.P., 2013. Plastic degradation and its environmental implications with special reference to poly (ethylene terephthalate). Polymers 5, 1–18. https://doi.org/10.3390/polym5010001.